Hittite Journal of Science and Engineering, 2015, 2 (1) 115-125
ISSN NUMBER: 2149-2123
DOI: 10.17350/HJSE19030000013

# A Second Degree Newton Method for an Inverse Scattering Problem for a Dielectric Cylinder

**Ahmet Altundag**
Istanbul Sabahattin Zaim University, Department of Mathematics Education, Istanbul, TURKEY

ABSTRACT

The inverse obstacle scattering problem we are interested is to reconstruct the image of an infinitely long homogeneous dielectric cylinder from the far field pattern for scattering of a time-harmonic E-polarized electromagnetic plane wave. We extend the approach suggested by Kress and Lee [18] that combines the ideas of Hettlich and Rundell [10] and Johansson and Sleeman [14] for the case of the inverse problem for a perfectly conducting scatterer to the case of penetrable scatterer. The inverse problem is depended on a system of non-linear boundary integral equations associated with a single layer approach to solve the direct scattering problem. We show the mathematical foundations of the method and illustrate its feasibility by numerical examples.

**Key Words:**
Helmholtz Equation; Inverse Scattering; Transmission Boundary Condition; Non-Linear Integral Equations; Gauss-Newton Iteration Methods; Single-Layer Approach.

***Article History:***
*Received: 2015/05/17*
*Accepted: 2014/06/12*
*Online: 2015/07/01*

***Correspondence to**: Ahmet Altundag, Istanbul Sabahattin Zaim University, Faculty of Engineering and Natural Sciences, Department of Mathematics Education, Istanbul, Turkey*
*Tel: +90 (212) 692-9738*
*Fax: +90 (212) 693-8229*
*E-Mail: ahmet.altundag@izu.edu.tr*

## INTRODUCTION

Inverse scattering theory is concerned with methods for retrieving information on the geometry and the physical properties of obstacles from scattering of acoustic and electromagnetic wave. In the direct scattering problem the object is given and it is required to find the scattered wave. In the inverse scattering problem we want to receive information on geometry of the shape or physical parameters of the scattering object.

The inverse obstacle scattering problem that we currently deal with is considered for time-harmonic waves. The scattering object is assumed to be a homogeneous scatterer and the inverse problem is to reconstruct an image of the scatterer. In this manuscript we are interested in dielectric obstacles and restrict ourselves to the sufficiently long cylinders. This constrain provides us to reduce the inverse scattering problem into two dimensions.

Let simply connected bounded domain $D$ be subset of $\mathbb{R}^2$ with $C^2$ boundary $\Gamma$. It illustrates the cross section of a sufficiently long dielectric cylinder and has constant wave number $k_d$ with real and imaginary part larger than zero. $k_0$ and $\nu$ denote the exterior positive wave number and the outward unit normal to the boundary $\Gamma$. For a given one or several incident fields $v^i(x) = e^{ik_0 x\cdot d}$ with incident direction $d$ defined as a unit vector, for $E$ –polarized electromagnetic waves the forward problem is assembled by the following Helmholtz equation with the transmission boundary condition: We look for solutions $v \in H^1_{loc}(\mathbb{R}^2 \setminus \bar{D})$ and $w \in H^1(D)$ to satisfy the Helmholtz equations

$$\Delta v + k_0^2 v = 0 \quad \text{in } \mathbb{R}^2 \setminus \bar{D}, \quad \Delta w + k_d^2 w = 0 \quad \text{in } D \tag{1.1}$$

fulfilling the transmission conditions

$$v = w, \quad \frac{\partial v}{\partial \nu} = \frac{\partial w}{\partial \nu} \quad \text{on } \Gamma \tag{1.2}$$

in the trace sense such that $v = v^i + v^s$. To ensure the scattered wave $v^s$ vanishes at infinity, it requires to fulfil the following radiation condition

$$\lim_{r\to\infty} r^{1/2}\left(\frac{\partial v^s}{\partial r} - ik_0 v^s\right) = 0, \quad r = |x|. \tag{1.3}$$

It uniformly holds in all directions. The radiation condition can be rewritten as an asymptotic behaviour of the form

$$v^s(x) = \frac{e^{ik_0|x|}}{\sqrt{|x|}}\left\{v_\infty\left(\frac{x}{|x|}\right) + O\left(\frac{1}{|x|}\right)\right\}, \quad |x| \to \infty. \tag{1.4}$$

The $v_\infty$ is an analytic function defined on the unit circle $S^1$ in $\mathbb{R}^2$ and is known far-field pattern of scattered field (see[8]).

The inverse obstacle scattering problem we are interested in is to reconstruct the boundary $\Gamma$ of the scattering dielectric $D$ by knowing $v_\infty$ for one or several incident fields with different incident direction $d \in S^1$.

At this point we note that uniqueness results for this inverse transmission problem are only available for the case of infinitely many incident waves (see [15]). A general uniqueness result based on the far field pattern for one or finitely many incident waves is still lacking. More recently, a uniqueness result for recovering a dielectric disk from the far-field pattern for scattering of one incident field was established by Altundag and Kress [2].

For a more stable and accurate solution of the inverse transmission problem we extend the approach suggested by Kress and Lee [18] that combines the ideas of Hettlich and Rundell [10] and Johansson and Sleeman [14] from the case of the inverse problem for an object that is perfect conductor to the case of the inverse problem for an object that penetrates the incident field.

In order to transform the forward problem (1.1)–(1.3) to boundary integral equation, we represent the solution $v^s$ and $w$ to the direct scattering obstacle problem in terms of single-layer potential in $\mathbb{R}^2 \setminus \bar{D}$ and in $D$ with the densities $\xi_0$ and $\xi_d$, respectively. Approaching the boundary and using the jump relation and transmission boundary condition (1.2) we obtain a system of two boundary integral equations on the boundary $\Gamma$ for the corresponding densities. We will denote this system of integral equations as a field equations. For the inverse obstacle scattering problem, the given far field pattern $v_\infty$ and the required coincidence ofthe far field of the single-layer potential provides a further equation. In the sequel, we will denote this equation as a data equation. Field and data equation can be considered as three equations for three unknowns, i.e., boundary curve and the two densities. The system of boundary integral equations is non-linear with respect to the boundary and linear with respect to the two densities.This system of integral equations is ill-posed. The ill-posedness of the inverse problem is reflected through the ill-posedness of the data equation. This open up variety approaches to solve the inverse scattering obstacle problem by linearization and iteration. The first approach applied in [2]. The idea of the approach described as follows: Given an approximation $\Gamma_{approx}$ for the boundary $\Gamma$ in a first step the well-posed field equations can be solved for two densities on $\Gamma_{approx}$. Then in a second step, keeping the densities fixed, the ill-posed field equation can be linearised with respect to the boundary and the solution of the ill-posed linearised equation can be utilized to update the boundary approximation. Because of the ill-posedness the solution of this update equation requires stabilization. These two steps can be iterated until some suitable stopping criterion is satisfied. The second approach implemented in [3]. From the spirit of [20], the iteration scheme constructed as follows: Given an approximation $\Gamma_{approx}$ for the boundary $\Gamma$ and approximations $\xi_{d,approx}$, $\xi_{0,approx}$ for the densities $\xi_d$ ,$\xi_0$ we linearize both the field and the data equations simultaneously with respect to the boundary curve and the two densities. The linear equations are then solved to update both the boundary curve and the two densities. Because of the ill-posedness the solution of the update equations requires stabilization, for example, by Tikhonov regularization. This procedure is then iterated until some suitable stopping criterion is achieved. In the current paper, the third approach is carried out. In the spirit of [10], [14] and [18], given an approximation $\Gamma_{\mathbf{approx}}$ for the boundary $\Gamma$ in a first step the well-posed field equations can be solved for two densities on $\Gamma_{\mathbf{approx}}$. Then in a second step, keeping the densities fixed, the ill-posed data equation can be linearised with respect to the boundary and we solve the linearised first degree data equation for a predictor. In a third step, keeping the densities fixed, we solve non-linear quadratic equation recursively for some steps to obtain a corrector. In a fourth step, we update the boundary approximation by $\Gamma_{\mathbf{approx}} + \mathbf{corrector}$ and continue this procedure until some suitable criteria is achieved. Because of the ill-posedness the solution of linearised data equation and quadratic equation require stabilization.

For a recent survey on the connections of the different approaches see Ivanyshyn, Kress and Serranho [12,13]. For related work for the Laplace equation we refer to Kress and Rundell [20] for the Dirichlet boundary condition and Eckel and Kress [9] Altundag and Kress [2,3] and Altundag [1,4] for the transmission condition and Altundag [5] for the transmision-impedance boundary condition. Finally, for a recent survey on the second degree Newton method see Hettlich and Rundell [10] Kress and Lee [18] Kress, Tezel and Yaman [22].

The scheme of the current manuscript is described as follows: In the second section we describe the solution of the forward problem via a single-layer potential approach as a base of our inverse algorithm. In the third section, we explain numerical solution of the forward algorithm. In the fourth section, the inverse algorithm is explained deeply. In the final section, we illustrate the feasibility of the method by demonstrating some numerical examples comparing the result with those for the Johansson and Sleeman method in [2], for the hybrid method in [4], and for the simultaneous linearization method in [3].

## The forward problem

The forward problem (1.1)–(1.3) has at most one solution (see [7,19] for the three-dimensional case). Existence of a solution can be seen [7,19] for the three-dimensional case. The solution of the forward scattering problem is established in [2]. The forward scattering problem is solved via single-layer potential approach. The fundamental solution to the Helmholtz equation is given by

$$\Phi_k(x,y) := \frac{i}{4} H_0^{(1)}(k|x-y|), \quad x \neq y,$$

where $k$ represents wave number and $H_0^{(1)}$ denotes the Hankel function of first kind and order zero. Using the notation of [8], in a Sobolev space setting, we introduce the single-layer potential operators

$$S_k : H^{-1/2}(\Gamma) \to H^{1/2}(\Gamma)$$

by

$$(S_k\xi)(x) := 2\int_\Gamma \Phi_k(x,y)\xi(y)\, ds(y), \quad x \in \Gamma, \tag{2.5}$$

and the normal derivative operators

$$K_k' : H^{-1/2}(\Gamma) \to H^{-1/2}(\Gamma)$$

by

$$(K_k'\xi)(x) := 2\int_\Gamma \frac{\partial \Phi_k(x,y)}{\partial \nu(x)}\, \xi(y)\, ds(y), \quad x \in \Gamma. \tag{2.6}$$

where $k = k_d$ and $k = k_0$. For the related mapping property, we cite to [17,23].

By using the jump relations on the boundary $\Gamma$, the single-layer potentials

$$\begin{aligned} w(x) &= \int_\Gamma \Phi_{k_d}(x,y)\xi_d(y)\, ds(y), \quad x \in D, \\ v^s(x) &= \int_\Gamma \Phi_{k_0}(x,y)\xi_0(y)\, ds(y), \quad x \in \mathbb{R}^2 \setminus \bar{D}, \end{aligned} \tag{2.7}$$

solve the forward problem (1.1)–(1.3) provided the densities $\xi_d$ and $\xi_0$ fulfil

$$\begin{aligned} S_{k_d}\xi_d - S_{k_0}\xi_0 &= 2v^i|_\Gamma, \\ \xi_d + \xi_0 + K_{k_d}'\xi_d - K_{k_0}'\xi_0 &= 2\left.\frac{\partial v^i}{\partial \nu}\right|_\Gamma. \end{aligned} \tag{2.8}$$

Provided $k_0$ is not a Dirichlet eigenvalue of the negative Laplacian for $D$, (2.7) has at most one solution. For the existence analysis and uniqueness of a solution, we refer to [2].

## Numerical solution of the forward problem

To solve (2.8) numerically and present the inverse algorithm we assume the boundary curve $\Gamma$ is defined by

$$\Gamma = \{\zeta(s) : 0 \le s \le 2\pi\}, \tag{3.1}$$

where $\zeta$ is a $2\pi$–periodic and smooth function. By $\chi = \xi \circ \zeta$ representing the dependence of the operators on the boundary curve, we introduce the parametrized single-layer operator

$$\tilde{S}_k : H^{-1/2}[0,2\pi] \times C^2[0,2\pi] \to H^{1/2}[0,2\pi]$$

by

$$\tilde{S}_k(\chi,\zeta)(s) := \frac{i}{2}\int_0^{2\pi} H_0^{(1)}\left(k|\zeta(s)-\zeta(\tau)|\right)|\zeta'(\tau)|\,\chi(\tau)\,d\tau$$

and the parametrized normal derivative operators

$$\tilde{K}'_k : H^{-1/2}[0,2\pi] \times C^2[0,2\pi] \to H^{-1/2}[0,2\pi]$$

by

$$\tilde{K}'_k(\chi,\zeta)(s) := \frac{ik}{2}\int_0^{2\pi} \frac{[\zeta'(s)]^{\perp}\cdot[\zeta(\tau)-\zeta(s)]}{|\zeta'(s)|\,|\zeta(s)-\zeta(\tau)|}\, H_1^{(1)}\left(k|\zeta(s)-\zeta(\tau)|\right)|\zeta'(\tau)|\,\chi(\tau)\,d\tau$$

for $s \in [0,2\pi]$. We made use of $H_0^{(1)\prime} = -H_1^{(1)}$ and $b^{\perp} = (b_2, -b_1)$ for any vector $b = (b_1, b_2)$. The parameterized form of (2.8) has the representation as follows

$$\begin{aligned} \tilde{S}_{k_d}(\chi_d,\zeta) - \tilde{S}_{k_0}(\chi_0,\zeta) &= 2\,v^i \circ \zeta, \\ \chi_d + \chi_0 + \tilde{K}'_{k_d}(\chi_d,\zeta) - \tilde{K}'_{k_0}(\chi_0,\zeta) &= \frac{2}{|\zeta'|}\,[\zeta']^{\perp}\cdot \operatorname{grad} v^i \circ \zeta. \end{aligned} \tag{3.2}$$

The kernels

$$A(s,\tau) := \frac{i}{2}\, H_0^{(1)}\left(k|\zeta(s)-\zeta(\tau)|\right)|\zeta'(\tau)|$$

and

$$B(s,\tau) := \frac{ik}{2}\,\frac{[\zeta'(s)]^{\perp}\cdot[\zeta(\tau)-\zeta(s)]}{|\zeta'(s)|\,|\zeta(s)-\zeta(\tau)|}\, H_1^{(1)}\left(k|\zeta(s)-\zeta(\tau)|\right)|\zeta'(\tau)|$$

of the operators $\tilde{S}_k$ and $\tilde{K}'_k$ can be written in the form

$$\begin{aligned} A(s,\tau) &= A_1(s,\tau)\ln\left(4\sin^2\frac{s-\tau}{2}\right) + A_2(s,\tau), \\ B(s,\tau) &= B_1(s,\tau)\ln\left(4\sin^2\frac{s-\tau}{2}\right) + B_2(s,\tau), \end{aligned} \tag{3.3}$$

where

$$A_1(s,\tau) := -\frac{1}{2\pi} J_0(k|\zeta(s)-\zeta(\tau)|)|\zeta'(\tau)|,$$

$$A_2(s,\tau) := A(s,\tau) - A_1(s,\tau)\ln\left(4\sin^2\frac{s-\tau}{2}\right),$$

$$B_1(s,\tau) := -\frac{k}{2\pi}\frac{[\zeta'(s)]^{\perp}\cdot[\zeta(\tau)-\zeta(s)]}{|\zeta'(s)|\,|\zeta(s)-\zeta(\tau)|} J_1(k|\zeta(s)-\zeta(\tau)|)\,|\zeta'(\tau)|,$$

$$B_2(s,\tau) := B(s,\tau) - B_1(s,\tau)\ln\left(4\sin^2\frac{s-\tau}{2}\right).$$

$J_0$ and $J_1$ denote the Bessel functions of order zero and one respectively. The functions $A_1, A_2, B_1$, and $B_2$ turn out to be analytic with diagonal terms

$$A_2(s,s) = \left[\frac{i}{2} - \frac{C}{\pi} - \frac{1}{\pi}\ln\left(\frac{k}{2}|\zeta'(s)|\right)\right]|\zeta'(s)|$$

in terms of Euler's constant $C$ and

$$B_2(s,s) = -\frac{1}{2\pi}\frac{[\zeta'(s)]^{\perp}\cdot\zeta''(s)}{|\zeta'(s)|^2}.$$

For the boundary integral equations with kernels of the form (3.3) a combined quadrature and collocation methods based on trigonometric interpolation, we refer to [8] or [21] and we also refer to [17] for the related error analysis.

To illustrate a numerical example, we examine the scattering of an incident field from a sufficiently long homogeneous dielectric cylinder. Its cross section consists of a non-convex kite-shaped and it is expressed by the parametric form

$$\zeta(s) = (\cos s + 0.65\cos 2s - 0.65, 1.5\sin s), \quad 0 \le s \le 2\pi. \tag{3.4}$$

The far-field pattern of the single-layer potential $v^s$ with density $\xi_0$ is given by

$$v_\infty(\hat{x}) = \alpha\int_\Gamma e^{-ik_0\hat{x}\cdot y}\,\xi_0(y)\,ds(y), \quad \hat{x}\in S^1, \tag{3.5}$$

where

$$\alpha = \frac{e^{i\frac{\pi}{4}}}{\sqrt{8\pi k_0}}.$$

Table 1 illustrates some numerical result for the far field pattern $v_\infty(d)$ with respect to forward direction $d$ and $v_\infty(-d)$ with respect to opposite direction $-d$. $d = (1,0)$ is chosen as a direction of incident field and the wave numbers are $k_0 = 1$ and $k_d = 2+3i$.

## The inverse problem

We progressed to explain an iterative scheme for solving the inverse obstacle scattering problem. We extend the inverse algorithm suggested by by Kress and Lee [18] that combines the ideas of Hettlich and Rundell [10] and Johansson and Sleeman [14] from the case of impenetrable scatterer to the case of penetrable scatterer. To do that it requires to introduce far-field operator of the form $S_\infty: H^{-1/2}(\Gamma) \to L^2(S^1)$ by

$$(S_\infty\xi)(\hat{x}) := \alpha\int_\Gamma e^{-ik_0\hat{x}\cdot y}\,\xi(y)\,ds(y), \quad \hat{x}\in S^1. \tag{4.1}$$

By considering the equations (2.7) and (3.5) we deduce that far-field pattern for the solution to forward problem

$$v_\infty = S_\infty\xi_0 \tag{4.2}$$

in terms of the solution to (2.8). Now, we can state the following theorem as a basis of inverse scattering problem.

**Theorem 4.1.** Assume that far-field pattern $v_\infty$ and an incident plane wave $v^i$ are given. Assume $\xi_d$ and $\xi_0$, the boundary curve $\Gamma$ fulfil the following equations

$$\begin{aligned} S_{k_d}\xi_d - S_{k_0}\xi_0 &= 2v^i, \\ \xi_d + \xi_0 + K'_{k_d}\xi_d - K'_{k_0}\xi_0 &= 2\frac{\partial v^i}{\partial v}, \\ S_\infty\xi_0 &= v_\infty. \end{aligned} \tag{4.3}$$

**Table 1.** Approximate numerical value for the forward scattering problem

| $n$ | Real $[v_\infty(d)]$ | Imag $[v_\infty(d)]$ | Real $[v_\infty(-d)]$ | Imag $[v_\infty(-d)]$ |
|---|---|---|---|---|
| 8 | -0.6017247940 | -0.0053550779 | -0.2460323014 | 0.3184957768 |
| 16 | -0.6018967551 | -0.0056192337 | -0.2461831740 | 0.3186052686 |
| 32 | -0.6019018135 | -0.0056277492 | -0.2461946976 | 0.3186049949 |
| 64 | -0.6019018076 | -0.0056277397 | -0.2461946846 | 0.3186049951 |

Then boundary curve $\Gamma$ solves the inverse obstacle scattering problem.

The system of boundary integral equations (4.3) is linear with respect to the densities and non-linear with respect to the boundary curve $\Gamma$. What is more, it is ill-posed. The ill-posedness of the inverse problem is reflected through the ill-posedness of the third integral equation, the far field equation denoted as *data equation*. In the current paper, we are going to proceed as follows: Given a current approximation $\Gamma_{\mathbf{approx}}$ for $\Gamma$ in a first step the well-posed *field equations* can be solved for two densities on $\Gamma_{\mathbf{approx}}$. Then in a second step, keeping the densities fixed, the ill-posed *data equation* can be linearised with respect to the boundary curve and we solve the linearised first degree data equation for *a predictor*. In a third step, keeping the densities fixed, we solve non-linear quadratic equation recursively for some steps to obtain a *corrector*. In a fourth step, we update the boundary approximation by $\Gamma_{\mathbf{approx}} + corrector$. To describe the procedure in more detail, we also require the parametrized version

$$\tilde{S}_\infty : H^{-1/2}[0,2\pi] \times C^2[0,2\pi] \to L^2(S^1)$$

of the far field operator as given by

$$\tilde{S}_\infty(\chi,\zeta)(\hat{x}) := \gamma \int_0^{2\pi} e^{-ik_0 \hat{x}\cdot\zeta(\tau)} |\zeta'(\tau)|\chi(\tau)\, d\tau, \quad \hat{x} \in S^1. \tag{4.4}$$

Then the parametrized form of (4.3) is transformed of the form

$$\begin{aligned} \tilde{S}_{k_d}(\chi_d,\zeta) - \tilde{S}_{k_0}(\chi_0,\zeta) &= 2\, v^i \circ \zeta, \\ \chi_d + \chi_0 + \tilde{K}'_{k_d}(\chi_d,\zeta) - \tilde{K}'_{k_0}(\chi_0,\zeta) &= \frac{2}{|\zeta'|}\, [\zeta']^\perp \cdot \mathrm{grad}\, v^i \circ \zeta, \\ \tilde{S}_\infty(\chi_0,\zeta) &= v_\infty. \end{aligned} \tag{4.5}$$

For a fixed $\chi$ the Fréchet derivative $\tilde{S}'_\infty$ of the operator $\tilde{S}_\infty$ with respect to the boundary curve $\zeta$ in the direction $h_1$ is given by

$$\tilde{S}'_\infty(\chi,\zeta;h_1)(\hat{x}) := \alpha \int_0^{2\pi} e^{-ik_0 \hat{x}\cdot\zeta(\tau)} \left[ -ik_0\, \hat{x}\cdot h_1(\tau)|\zeta'(\tau)| + \frac{\zeta'(\tau)\cdot h_1'(\tau)}{|\zeta'(\tau)|} \right] \chi(\tau)\, d\tau \tag{4.6}$$

for $\hat{x} \in S^1$. Then the linearization of the third equation in (4.5) at $\zeta$ with respect to the direction $h_1$ reads

$$\tilde{S}_\infty \chi_0 + \tilde{S}'_\infty(\chi_0,\zeta;h_1) = v_\infty. \tag{4.7}$$

(4.7) is a linear equation for the predictor $h_1$ but it is ill-posed. The ill-posedness is inherited from Fréchet derivative of the boundary.

For a fixed $\chi$ the Fréchet derivative $\tilde{S}''_\infty$ of the operator $\tilde{S}'_\infty$ with respect to the boundary curve $\zeta$ in the direction $h_2$ can be deduced of the form

$$\tilde{S}''_{\infty}(\chi,\zeta;h_1,h_2)(\hat{x}) := \alpha \int_0^{2\pi} e^{-ik_0\,\hat{x}\cdot\zeta(\tau)} \{-k_0^2\,\hat{x}\cdot h_1(\tau)\,\hat{x}\cdot h_2(\tau)\;|\zeta'(\tau)| - ik_0\,\hat{x}\cdot h_2(\tau)\frac{\zeta'(\tau)\cdot h_1'(\tau)}{|\zeta'(\tau)|} - ik_0\,\hat{x}\cdot h_1(\tau)\frac{\zeta'(\tau)\cdot h_2'(\tau)}{|\zeta'(\tau)|} + \frac{h_1'(\tau)\cdot h_2'(\tau)}{|\zeta'(\tau)|} - \frac{\zeta'(\tau)\cdot h_1'(\tau)\;\zeta'(\tau)\cdot h_2'(\tau)}{|\zeta'(\tau)|^3}\Big\}\chi(\tau)d\tau. \tag{4.8}$$

Using the second degree approximation the equation (4.7) is replaced by the quadratic equation

$$S'_{\infty}(\chi,\zeta;h) + \frac{1}{2}S''_{\infty}(\chi,\zeta;h,h) = u_{\infty} - S_{\infty}(\chi,\zeta). \tag{4.9}$$

As in the inspire of Hettlich and Rundell [10], the nonlinear quadratic equation (4.9) is solved in two steps, namely a predictor and a corrector step. The predictor step coincides with the Johansson and Sleeman method [14]. For this step, we solve ill-posed linearized data equation (4.7) via Tikhonov regularization with Sobolev penalty term $H^p$ and regularization parameter $\lambda_{1,n}$ to obtain a predictor $h_1$. After $h_1$ obtained , in the corrector step the ill-posed linear equation can be expressed as follows

$$S'_{\infty}(\chi,\zeta;h_{j+1}) + \frac{1}{2}S''_{\infty}(\chi,\zeta;h_{j+1},h_j) = v_{\infty} - S_{\infty}(\chi,\zeta). \tag{4.10}$$

Equation(4.10) is solved recursively for $h_{j+1}, j = 1,\dots,M$ . Since equation(4.10) is ill-posed, it requires stabilization. We use Tikhonov regularization with Sobolev penalty term $H^p$ and regularization parameter $\lambda_{2,n}$.

Now, we can describe the algorithm as follows: given an approximation for the boundary curve $\Gamma$ with parametrization $\zeta$, each iteration step of the proposed inverse algorithm consists of fourth parts.

1. We solve the first two well-posed equations of (4.5), i.e., the field equations for the densities $\chi_d$ and $\chi_0$.
2. Keeping $\chi_0$ fixed, we solve the ill-posed linearized data equation (4.7) for a predictor $h_1$. Since the kernels of the integral operators in (4.7) are smooth, for its numerical approximation the composite trapezoidal rule can be employed. Because of the ill-posedness the solution of (4.7) requires stabilization, for example, by Tikhonov regularization.
3. Keeping $\chi_0$ fixed, we solve the linearized second degree equation (4.10) via Tikhonov regularization recursively in $M$ steps to obtain the corrector $h = h_{M+1}$.
4. We update the boundary approximation by $\zeta + h$ and return to first step until some suitable criteria is achieved. The following stopping criterion is implemented and it is given by the relative error

$$\frac{\| v_{\infty;N} - v_{\infty} \|}{\| v_{\infty} \|} \le \epsilon(\delta) \tag{4.11}$$

where $v_{\infty;N}$ is the computed far field pattern for after $N$ iteration steps and where $\epsilon(\delta) = \gamma\delta$, for noise level $\delta$ and $\gamma \approx 1$.

We represent the boundary parametrization of the form

$$\zeta(s) = p(s)\begin{pmatrix}\cos s\\ \sin s\end{pmatrix}, \quad 0 \le s \le 2\pi, \tag{4.12}$$

with a non-negative function $p$. The increments are of the form

$$h(s) = q(s)\begin{pmatrix}\cos s\\ \sin s\end{pmatrix}, \quad 0 \le s \le 2\pi, \tag{4.13}$$

with a real function $q$. For the approximation procedure, we assume that $p$ and its update $q$ have the form of a trigonometric polynomial of degree $J$,

$$q(s) = \sum_{j=0}^{J} a_j \cos js + \sum_{j=1}^{J} b_j \sin js. \tag{4.14}$$

The linearised equations (4.7) and (4.10) are solved in the least squares sense, penalized via Tikhonov regularization, for the unknown coefficients $a_0,\dots,a_J$ and $b_1,\dots,b_J$ of the trigonometric polynomial representing the update $q$. From the our numerical example, we observe that it is more advantageous to use an $H^p$ Sobolev penalty term rather than an $L^2$ penalty term in the Tikhonov regularization.

We interpret the operators $\tilde{S}'_\infty$ and $\tilde{S}''_\infty$ as an ill-posed linear operator having the mapping properties of form

$$\tilde{S}'_\infty,\ \tilde{S}''_\infty : H^p[0,2\pi] \to L^2[0,2\pi] \tag{4.15}$$

for some small $p \in \mathbf{IN}$.

As a theoretical basis for the application of Tikhonov regularization we refer to [11]. Under the assumption of star-like boundaries, the operator $\tilde{S}'_\infty$ and $\tilde{S}''_\infty$ are injective if $k_0^2$ is not a Neumann eigenvalue for the negative Laplacian in $D$.

We also extend the above algorithm for finitely many incident plane waves. Let $v_1^i, \dots, v_R^i$ are $R$ incident plane waves with different incident directions and $v_{\infty,1}, \dots, v_{\infty,R}$ be the corresponding far-field patterns for scattering from $\Gamma$. The inverse scattering problem is to reconstruct the unknown $\Gamma$. This is equivalent to solve

$$\begin{aligned} \tilde{S}_{k_d}(\chi_{d,r},\zeta) - \tilde{S}_{k_0}(\chi_{0,r},\zeta) &= 2\, v_r^i \circ \zeta, \\ \chi_{d,r} + \chi_{0,r} + \tilde{K}'_{k_d}(\chi_{d,r},\zeta) - \tilde{K}'_{k_0}(\chi_{0,r},\zeta) &= \frac{2}{|\zeta'|}\,[\zeta']^\perp \cdot \operatorname{grad} v_r^i \circ \zeta, \\ \tilde{S}_\infty(\chi_{0,r},\zeta) &= v_{\infty,r}, \end{aligned} \tag{4.16}$$

for $r = 1, \dots, R$. The inverse algorithm can be described as follows: Given an approximation $\zeta$, we firstly solve the first two equations in (4.16) for $r = 1, \dots, R$ to obtain $2R$ densities $\chi_{d,1}, \cdots, \chi_{d,R}$ and $\chi_{0,1}, \cdots, \chi_{0,R}$. Secondly, we solve the linearised equation

$$\tilde{S}_\infty \chi_{0,r} + \tilde{S}'_\infty(\chi_{0,r},\zeta;h_1) = v_{\infty,r}, \quad r = 1,\dots,R, \tag{4.17}$$

for the predictor $h_1$ by interpreting them as one ill-posed equation with an operator from $H^p[0,2\pi] \mapsto (L^2[0,2\pi])^R$ and applying Tikhonov regularization. Thirdly we solve linearized second degree equation

$$S'_\infty(\chi_{0,r},\zeta;h_{j+1}) + \frac{1}{2}S''_\infty(\chi_{0,r},\zeta;h_{j+1},h_j) = v_{\infty,r} - S_\infty(\chi_{0,r},\zeta) \tag{4.18}$$

**Numerical examples**

As proof of concept rather than a documentation of a fully developed code, in this final section we present some numerical examples exhibiting the feasibility of our approach. In order to prevent an inverse crime, the synthetic far-field data were obtained by using the boundary integral equations based on a combined single- and double layer potential approach (see [7,19]). We use the numerical algorithm explained in [8,17,16] 64 quadrature points are used. The linearised data equation (4.7) and linearised second degree data equation (4.10) were solved by Tikhonov regularization with an $H^2$ penalty term, i.e., $p=2$ in (4.15). The regularized equation is solved by Nyström's method with the composite trapezoidal rule. The table 5.2 illustrates the types of contour given by corresponding representation formula.

In all our five examples we used R=8 as a number of incident waves with the directions d=(cos(2πr/R), sin(2πr/R), r=1,..., R and **J=10** as degree for the approximating trigonometric polynomials in (4.14) and M=10 as the number of recursion and the wave numbers $k_0$=1 and $k_d$=5 + 1i. The initial guess is given by the dotted line, the exact boundary curves are given by the dashed (blue) lines and the reconstructions by the full (red) lines. For simplicity, for the stopping rule we chose ε (σ) the same for all noise levels since this already gave satisfactory reconstructions. In according with the general convergence results on regularized Gauss–Newton method (see [6]) for the regularization parameters we used decreasing sequences

$$\lambda_{1,n} = \tau_1^{-n}\lambda_1, \qquad \lambda_{2,n} = \tau_2^{-n}\lambda_2$$

with $\lambda_1$, $\lambda_2$ positive and $\tau_1$, $\tau_2 > 1$ chosen by trial and error. The iteration numbers and the regularization parameters $\lambda_1$ and $\lambda_2$ for the Tikhonov regularization of (4.7) and (4.10), respectively, were chosen by trial and error. However, to illustrate the feasibility and stability of our method we used the same regularization parameter in all examples. These were chosen as $\lambda_1 = 0.9,\ \tau_1 = 1.2$ and $\lambda_2 = 0.8,\ \tau_2 = 1.36$.

Random errors are obtained by

$$\tilde{v}_\infty = v_\infty + \delta\eta\frac{\|v_\infty\|}{|\eta|} \tag{5.1}$$

**Table 2.** Boundary Curves

| *Types* | | *Representations* |
|---|---|---|
| *Dropped-shaped* | : | $\zeta(s) = \{(-0.5 + 0.75\sin\frac{s}{2}, -0.75\sin s) : s \in [0,2\pi]\}$ |
| *Apple-shaped* | : | $\zeta(s) = \{\frac{0.5+0.4\cos s+0.1\sin 2s}{1+0.7\cos s}(\cos s, \sin s) : s \in [0,2\pi]\}$ |
| *Kite-shaped* | : | $\zeta(s) = \{(\cos s + 1.3\cos^2 s - 1.3, 1.5\sin s) : s \in [0,2\pi]\}$ |
| *Peanut-shaped* | : | $\zeta(s) = \{\sqrt{\cos^2 s + 0.25\sin s}\ (\cos s, \sin s) : s \in [0,2\pi]\}$ |
| *Rounded triangle* | : | $\zeta(s) = \{(2 + 0.3\cos 3s)(\cos s, \sin s) : s \in [0,2\pi]\}$ |

with the random variable $\eta \in \mathbb{C}$ and $\{\mathrm{Re}\ \eta, \mathrm{Im}\ \eta\} \in (0,1)$.

In the first Figure 1, second Figure 2, third Figure 3, fourth Figure 4, and fifth Figure 5 examples illustrate reconstructions obtained after 13, 15, 15, 10, and 15 iterations respectively.

Table 3 illustrates the convergence behaviour of the proposed algorithm. The first column represents iteration number N and the other columns represent relative error determined by (4.11) for each contour 5.2.

Our examples clearly indicate the feasibility of the proposed algorithm with a reasonable stability against noise. From our further numerical experiments it is observed that using more than one incident wave improved on the accuracy of the reconstruction and the stability.

Furthermore, an appropriate initial guess is important to ensure numerical convergence of the iterations. Our examples also indicate that the proposed algorithm with the numerical reconstructions are superior to those obtained via by Johonsson and Sleeman method [14] in [2] to those obtained via by the hybrid method in [4]. Moreover, the proposed algorithm has as the same efficiency of accuracy and stability as the simultaneous linearization method in [3]. However, the proposed algorithm requires less computational effort than the simultaneous linearization method. Therefore, it is superior the simultaneous linearization method with respect to computational cost.


## ACKNOWLEDGEMENTS

The author thanks Professor Rainer Kress for the discussion on the topic of this paper.


**Table 3.** Relative error at each iteration step

| *N* | *Apple-Sh.* | *Dropped-Sh.* | *Kite-Sh.* | *Peanut-Sh.* | *R. Triangel* |
|---|---|---|---|---|---|
| 1 | 0.6757221101 | 0.6360551737 | 0.6368500557 | 0.2148574440 | 0.8949045371 |
| 2 | 0.1643964696 | 0.1657433896 | 0.2976995503 | 0.0503726493 | 0.3733278852 |
| 3 | 0.0422092172 | 0.0281626370 | 0.1881878713 | 0.0067460381 | 0.2176997240 |
| 4 | 0.0142325900 | 0.0161566231 | 0.1346324897 | 0.0025621311 | 0.0940590296 |
| 5 | 0.0096240121 | 0.0137267005 | 0.1076783088 | 0.0024559183 | 0.0415419160 |
| 6 | 0.0081622629 | 0.0124983950 | 0.0910946349 | 0.0023434131 | 0.0205255193 |
| 7 | 0.0062161463 | 0.0114739054 | 0.0796446254 | 0.0022429730 | 0.0115610162 |
| 8 | 0.0043983846 | 0.0105610342 | 0.0710851110 | 0.0021531523 | 0.0078191797 |
| 9 | 0.0031519393 | 0.0098295139 | 0.0643294142 | 0.0020709805 | 0.0062761911 |
| 10 | 0.0024892871 | 0.0093579625 | 0.0587910366 | 0.0019941389 | 0.0055382041 |
| 11 | 0.0021832518 | 0.0091470771 | 0.0541263151 | Terminated | 0.0050712243 |
| 12 | 0.0020280692 | 0.0091156042 | 0.0501207838 | | 0.0047028951 |
| 13 | 0.0019307739 | 0.0091655215 | 0.0466334592 | | 0.0043807490 |
| 14 | Terminated | 0.0092326307 | 0.0435672694 | | 0.0040879823 |
| 15 | | 0.0092904674 | 0.0408523510 | | 0.0038178513 |
| 16 | | Terminated | Terminated | | Terminated |

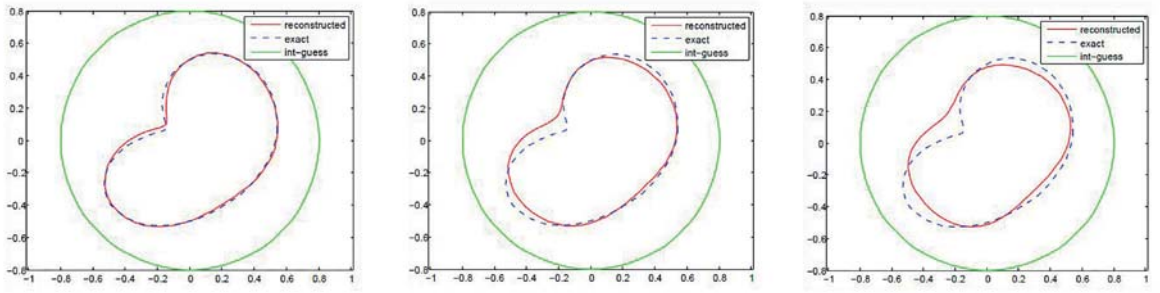


**Figure 1.** Reconstruction of the apple-shaped contour 5.2 for exact data (left), 3% noise (middle) and 5% noise (right)

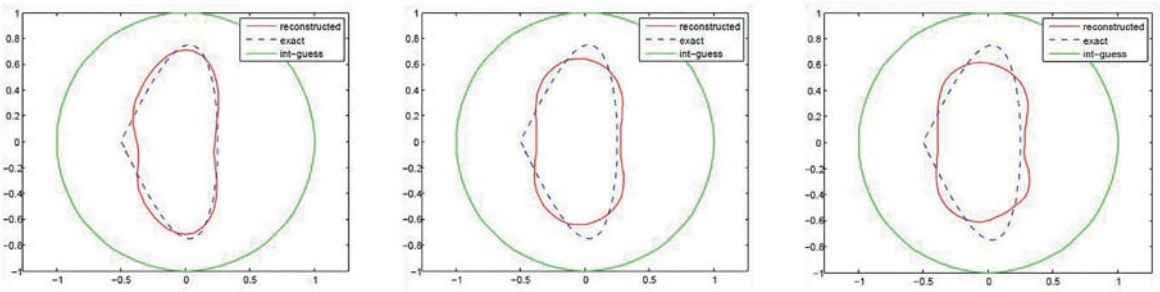


**Figure 2.** Reconstruction of dropped-shaped contour 5.2 for exact data (left), 3% noise (middle) and 5% noise (right)

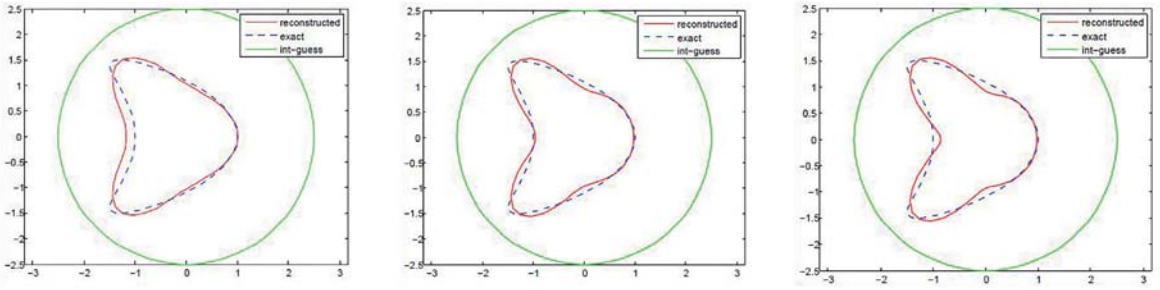


**Figure 3.** Reconstruction of kite-shaped contour 5.2 for exact data (left), 3% noise (middle) and 5% noise (right)

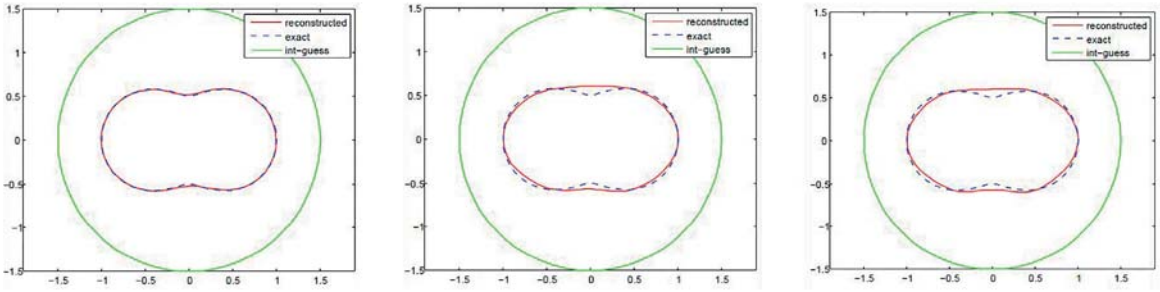


**Figure 4.** Reconstruction of peanut-shaped contour 5.2 for exact data (left), 3% noise (middle) and 5% noise (right)

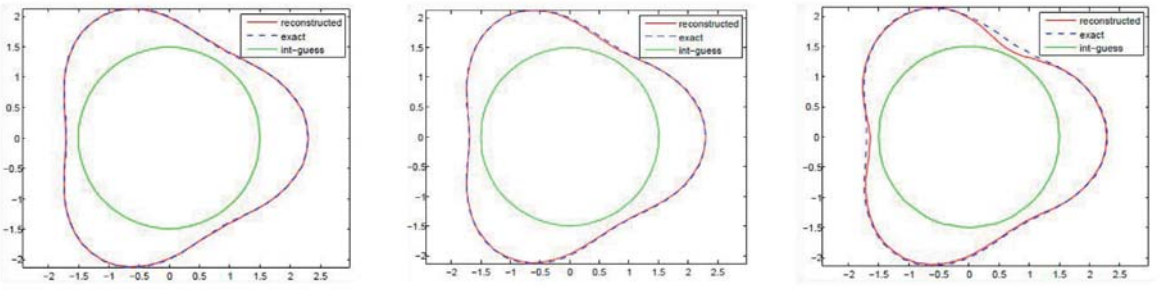


**Figure 5.** Reconstruction of rounded-triangle-shaped contour 5.2 for exact data (left), 3% noise (middle) and 5% noise (right)

## REFERENCES


1. Altundag, A. : *On a two-dimensional inverse scattering problem for a dielectric*. Dissertation, Göttingen, February 2012.
2. Altundag, A. and Kress, R. : *On a two dimensional inverse scattering problem for a dielectric*. Applicable Analysis, , 757–771 (2012).
3. Altundag, A. and Kress, R.: *An Iterative Method for a Two-Dimensional Inverse Scattering Problem for a Dielectric*. Jour. On Inverse and Ill–Posed Problem , pp. 575–590 (2012).
4. Altundag, A. : *A hybrid method for inverse scattering problem for a dielectric*. Advances in Applied Mathematics and Approximation Theory, Springer, , pp. 185–203 (2013).
5. Altundag, A. : *Inverse obstacle scattering with conductive boundary condition for a coated dielectric cylinder*. J. Concrete And Applicable Mathematics, , pp. 11–22 (2015).
6. Burger, M., Kaltenbacher, B., and Neubauer, A. : *Iterative Solution Methods*. Handbook of Mathematical Methods in Imaging (Scherzer, ed.) Springer, Berlin 345–384 (2011).
7. Colton, D. and Kress, R.: *Integral Equation Methods in Scattering Theory*. Wiley–Interscience Publications, New York 1983.
8. Colton, D. and Kress, R.: *Inverse Acoustic and Electromagnetic Scattering Theory*. 2nd. ed. Springer, Berlin 1998.
9. Eckel, H. and Kress, R.: *Non-linear integral equations for the inverse electrical impedance problem*. Inverse Problems , 475–491 (2007).
10. Hettlich, F. and Rundell, W.: *A second degree method for non-linear inverse problem*. SIAM J. Numer. Anal. , 587–620 (2000).
11. Ivanyshyn, O. and Johansson, T.: Boundary integral equations for acoustical inverse sound–soft scattering. J. Inverse Ill–Posed Probl. , 1–14 (2007).
12. Ivanyshyn, O. and Kress, R.: Non–linear integral equations in inverse obstacle scattering. In: *Mathematical Methods in Scattering Theory and Biomedical Engineering* (Fotiatis, Massalas, eds). World Scientific, Singapore, 39–50 (2006).
13. Ivanyshyn, O., Kress, R. and Serranho, R.: Huygens' principle and iterative methods in inverse obstacle scattering. Advances in Computational Mathematics , 413–429 (2010).
14. Johansson, T. and Sleeman, B.: Reconstruction of an acoustically sound–soft obstacle from one incident field and the far–field pattern. IMA Jour. Appl. Math. , 96–112 (2007).
15. Kirsch, A. and Kress, R.: Uniqueness in inverse obstacle scattering. Inverse Problems , 285–299 (1993).
16. Kress, R.: On the numerical solution of a hypersingular integral equation in scattering theory. J. Comp. Appl. Math., 345–360 (1995).
17. Kress, R.: *Integral Equations*. 2nd. ed Springer Verlag, Berlin 1998.
18. Kress, R. and Lee, K.M. : *A second degree Newton method for an inverse obstacle scattering problem* J. Comp. Phys. 7661–7669 (2011).
19. Kress, R. and Roach, G.F.: Transmission problems for the Helmholtz equation. J. Math. Phys. , 1433–1437 (1978) .
20. Kress, R. and Rundell, W.: Non–linear integral equations and the iterative solution for an inverse boundary value problem. Inverse Problems , 1207–1223 (2005).
21. Kress, R. and Sloan, I.H.: On the numerical solution of a logarithmic integral equation of the first kind for the Helmholtz equation. Numerische Mathematik , 199–214 (1993).
22. Kress, R., Tezel, N., and Yaman, F. : A second order Newton Method for sound soft inverse obstacle scattering. J. Inverse and Ill–posed Problems , 173–185 (2009).
23. McLean, W.: Strongly Elliptic Systems and Boundary Integral Equations. Cambridge University Press 2000.